JACS
JOURNAL OF THE AMERICAN CHEMICAL SOCIETY
Article
Cite This: J. Am. Chem. Soc. 2019, 141, 15827−15839
pubs.acs.org/JACS

Mechanism-Enabled Population Balance Modeling of Particle Formation en Route to Particle Average Size and Size Distribution Understanding and Control

Derek R. Handwerk,[†] Patrick D. Shipman,*[,†] Christopher B. Whitehead,[‡] Saim Özkar,[§] and Richard G. Finke*[,‡]

[†]Department of Mathematics and [‡]Department of Chemistry, Colorado State University, Fort Collins, Colorado 80523, United States

[§]Department of Chemistry, Middle East Technical University, 06800 Ankara, Turkey

Supporting Information

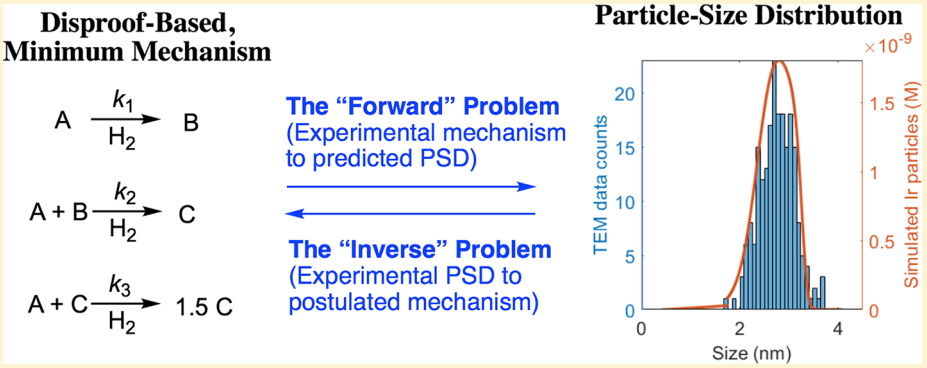

ABSTRACT: The concept of Mechanism-Enabled Population Balance Modeling (ME-PBM) is reported, illustrated by its application to a prototype $Ir(0)_n$ nanoparticle formation reaction. ME-PBM is defined herein as the use of now available, experimentally established, disproof-based, deliberately minimalistic mechanisms of particle formation as the required input for more rigorous Population Balance models, critically including an experimentally established nucleation mechanism. ME-PBM achieves the long-sought goal of connecting such now available experimental minimum mechanisms to the understanding and rational control of particles size and size distributions. Twelve pseudoelementary step, particle-formation mechanisms are considered so that the approach to the ME-PBM is also extensively disproof-based. Resurrection of Smoluchowski's 1918 full Ordinary Differential Equation (ODE) approach to the PBM is another, critical aspect of our approach which, in turn, allows unbiased *fitting* of the information-laden *particle-size distribution* (PSD) including its *shape*. The results provide one solution to the "inverse problem" in which the PSD informs one as to the correct particle formation mechanism: A new, deliberately minimalistic 3-step particle-formation mechanism has been uncovered that is a single-additional-step expansion of the now broadly used Finke−Watzky (FW) 2-step mechanism, the new 3-step mechanism being: A → B (rate constant k_1), A + B → C (rate constant k_2), and A + C → 1.5C (rate constant k_3), where A represents the monomeric nanoparticle precursor, B represents "small" nanoparticles, and C represents "larger" nanoparticles. The results strongly support three paradigm shifts for nucleation and growth of particles, the most critical paradigm shift being that the "burst" nucleation assumption in LaMer's 1950s model of particle formation is *not* required to produce narrow, near-monodisperse PSDs. Instead, narrow PSDs can be and are achieved despite continuous nucleation because *smaller particles grow faster than larger ones, $k_2 > k_3$, thereby allowing the smaller particles to catch up in size to the more slowly growing larger particles.*

1. INTRODUCTION

The physical properties and applications of catalyst[1,2] and other particles[3−7] typically depend strongly on their size and size distributions. Because of this, a long-standing goal, if not "Holy Grail," in nanoparticles and other particle science across nature has been the rational, mechanism-guided synthesis of nanoparticles and other particles with desired size and narrow particle size distributions (PSDs). However, reliable chemical-mechanism-based particle syntheses with size and size distribution control have to date proved extremely elusive. This is because five required components were previously unavailable and, therefore, previously unassembled into the mathematical framework of population balance modeling (PBM):[8−13] (i) an experimentally established mechanism of the critical *nucleation step* to start off the particle synthesis

Received: June 14, 2019
Published: September 26, 2019

DOI: 10.1021/jacs.9b06364
J. Am. Chem. Soc. 2019, 141, 15827−15839

correctly; (ii) the experimentally established *minimum mechanisms* to test for the subsequent growth and any possible agglomeration steps; (iii) a solution to the "forward" problem of coupling of those mechanisms to the PSD in a way that not only simulates the PSD and its shape without an assumption of that PSD shape, but also (iv) grants the ability to *fit* the PSD and take into account the kinetic information-rich shape of the PSD. The key point to realize here is that the PSD is information-laden; it is a convolution of all of the kinetic information and events that led up to the observed PSD. Lastly and most importantly, (v) the fit-derived kinetics from the information-laden PSD then need, at least ideally, to be used to refine the proposed mechanism, that is, to suggest a solution for the always challenging "inverse" problem of using the "effects" (here the PSD) to inform and revise the implied "cause" (here the correct particle formation mechanism).

We have been able to achieve and assemble each of the above five missing components; the result is what we define herein as *Mechanism-Enabled* Population Balance Modeling (ME-PBM). ME-PBM developed and employed herein yields results that in turn strongly suggest *three paradigm shifts in the understanding of particle formation* that are described as follows: (1) Nucleation is hypothesized to more generally be *continuous*, as first discovered in 1997,[14] and not "instantaneous" or "burst" as the widely cited, but now disproven[15] LaMer model from the 1950s[16] asserts. (2) Nucleation is hypothesized to more generally be low molecularity[17,18] in strongly bonding, higher energy monomer systems (e.g., 2−3 as in the termolecular, Ir_3 kinetically effective nucleus (KEN)[17] herein) and not the higher molecularity implied by classical nucleation theory (CNT)[19−23] and its reversible assembly for weakly bonding systems, $n\mathrm{A} \rightleftarrows \mathrm{A}_n$ from more stable monomers. (3) Critically and as detailed herein for the first time, *autocatalytic growth of smaller particles is faster than that of larger particles. In this way the smaller particles therefore "catch up" in size with the more slowly growing larger ones*. This results in surprisingly narrow PSDs from self-assembly syntheses involving continuous nucleation and autocatalytic growth.[14]

The finding that smaller particles grow more quickly than larger ones is especially timely and significant, as it answers the previously perplexing question of "How can narrow size distributions result from self-assembly synthesis in the absence of the putative 'instantaneous' nucleation postulated by the 1950 LaMer model of particle formation?".[15] The *assumption* of "instantaneous", "burst" nucleation in the LaMer model, a mathematically necessary assumption at the time for LaMer's *growth model*,[15] has been cited more than 1953 times since 1950,[15] often to justify how narrow PSDs can be formed. A review of the literature citing the LaMer model reveals the remarkable insight that there is very little, if any, convincing experimental evidence for anything approaching "burst" nucleation in the 69 years since the LaMer model of particle *growth* first appeared.[15]

2. PROTOTYPE $Ir(0)_n$ NANOPARTICLE FORMATION SYSTEM EXAMINED

Scheme 1 shows the prototype $Ir(0)_n$ formation system examined herein which begins from the well-characterized and atomically precise[24,25] precursor and precatalyst $\{(1,5\text{-COD})Ir^{I}\cdot POM\}^{8-}$ (POM = the polyoxometalate, $P_2W_{15}Nb_3O_{62}^{9-}$). Reduction of this precursor under H_2 yields average-size $Ir(0)_{\sim 730}$ nanoparticles under the specific conditions employed herein. The $Ir(0)_{\sim 730}$ nanoparticles were

Scheme 1. Experimentally Determined, Balanced Reaction Stoichiometry for the Formation of $Ir(0)_{\sim 730}$ Nanoparticles

$$730\ [(1,5\text{-COD})Ir{\cdot}P_2W_{15}Nb_3O_{62}]^{8-} + 1825\ H_2 \longrightarrow Ir(0)_{\sim 730} + 730\ \text{cyclooctane} + 730\ H^+ + 730\ [P_2W_{15}Nb_3O_{62}]^{9-}$$

prepared from the $\{(1,5\text{-COD})Ir^{I}\cdot POM\}^{8-}$ (POM = $P_2W_{15}Nb_3O_{62}^{9-}$) precursor/precatalyst as in previous works.[14,24,25]

Scheme 2 shows the molecular level nucleation mechanism for the $\{(1,5\text{-COD})Ir^{I}\cdot POM\}^{8-}$ to $Ir(0)_n$ nanoparticle formation system based on work reported in 2017.[18] This so-termed "alternative termolecular nucleation"[18] mechanism (i.e., alternative to a mechanism net-third-order in the $\{(1,5\text{-COD})Ir^{I}\cdot POM\}^{8-}$ precatalyst) has proven critical to finding a mechanism-enabled PBModel that can quantitatively account for the observed PSD, *vide infra*. This upfront need for an experimentally determined nucleation mechanism makes intuitive and chemical sense given that nucleation sets the critical starting point and KEN[17] for the rest of the particle formation process.

In Scheme 2A, the $Ir(0)_n$ nanoparticles are formed from the molecular, well-characterized $\{(1,5\text{-COD})Ir^{I}\cdot POM\}^{8-}$ precursor, while in Scheme 2B, the A·L nomenclature has been applied where A·L = $\{[(1,5\text{-COD})Ir^{+}][POM^{9-}]\}^{8-}$.

Multiple different nucleation mechanisms were specifically considered, and disproved, in a prior 2017 publication[18] en route to the alternative nucleation mechanism shown in Scheme 2. The disproved nucleation mechanisms are (i) bimolecular in Ir (i.e., Ir_2); (ii) simple termolecular in Ir (Ir_3); and importantly (iii) all higher molecularity, $n > 3$, Ir_n, nucleation mechanisms.

Such experimentally determined, molecular-level mechanisms of nucleation are a rarely achieved but critical goal for each and every one of the myriad of phase-change processes across nature that involve nucleation.[26−30] Noteworthy here is the *paradigm shift* away from CNT that typically has been used (inappropriately; incorrectly!) in what are ultimately futile attempts to try to underpin PBM of particle formation in high-energy, low solubility, monomer systems that exhibit strong monomer−monomer bonding.[14,17,18,31] The paradigm shift is that instead *low molecularity, $n = 2-3$, $(monomer)_n$ nucleation*[14,17,18,31] with a KEN[17] of Ir_{2-3} is what starts off at least the $Ir(0)_{\sim 730}$ nanoparticle formation system examined herein, as in Scheme 2. Without such knowledge of the true, molecular mechanism of nucleation, one cannot possibly start off the PBM correctly except by accident—and will likely reach erroneous conclusions about the particle formation process as resulted in an otherwise valuable 2014 PBM study.[32]

3. NEXT REQUIREMENT FOR ME-PBM: EXPERIMENTALLY DETERMINED, MINIMALISTIC NANOPARTICLE FORMATION MECHANISMS WITH WHICH TO ENABLE PBM

The experimentally based, minimalistic nanoparticle-formation mechanisms required to enable population balance modeling in terms of pseudoelementary steps[14,33] (that themselves are just sums of true elementary steps),[14,33] have been developed deliberately and painstakingly over the past 26 years.[14,17,18,24,25,31,34−40] These deliberately minimalistic, extensively disproof-based[41,42] mechanisms are shown in Scheme 3. These mechanisms have primarily (albeit not exclusively)[35,36,38] been worked out for the prototype $Ir(0)_n$

DOI: 10.1021/jacs.9b06364
J. Am. Chem. Soc. 2019, 141, 15827−15839

Scheme 2. (A) Molecular-Level "Alternative Termolecular"[18] Mechanism of Nucleation of $Ir(0)_n$ Nanoparticle Formation and (B) Restatement of the Alternative Termolecular Mechanism in Terms of "A·L" Nomenclature

Part A:

$$2\,(COD)Ir{\bullet}POM^{8-} + 4\,solv \overset{K_{Diss}}{\rightleftharpoons} 2\,(COD)Ir(solv)_2^{+} + 2\,POM^{9-}$$

$$2\,(COD)Ir(solv)_2^{+} + (COD)Ir{\bullet}POM^{8-} + 7.5\,H_2 \xrightarrow{k_{1(alt.termol)}} 3Ir(0) = Ir(0)_3 + POM^{9-} + 3H^{+} + 3\,cyclooctane + 4\,solv$$

$$\text{Net:}\quad 3\,(COD)Ir{\bullet}POM^{8-} + 7.5\,H_2 \longrightarrow 3\,Ir(0) = Ir(0)_3 + 3\,POM^{9-} + 3H^{+} + 3\,cyclooctane$$

Part B:

$$2\{A{\bullet}L + 2\,solv \rightleftharpoons A(solv)_2 + L\}$$

$$2\,A(solv)_2 + A{\bullet}L \longrightarrow 3B(=B_3) + L + 4\,solv$$

$$\text{Net:}\quad 3\,A{\bullet}L \longrightarrow 3B(=B_3) + 3\,L$$

Scheme 3. Five Total, Experimentally Established Pseudoelementary Steps That Are Now Available for Mechanistically Enabling PB Models[14,34−40]

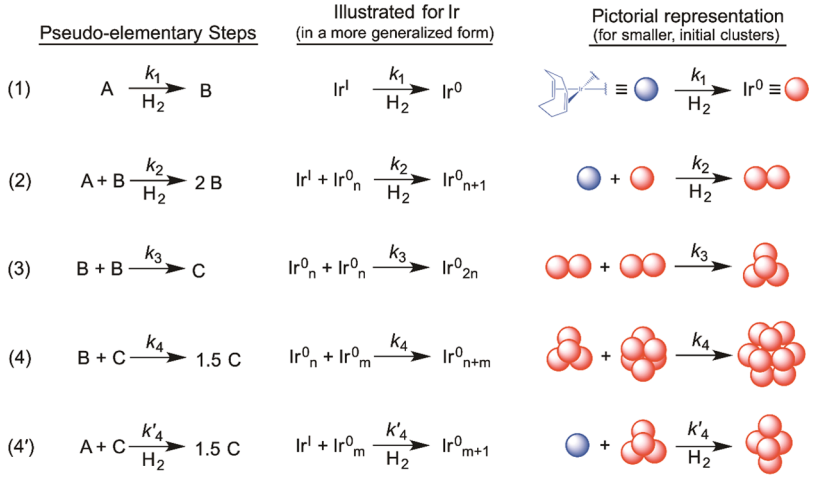

nanoparticle formation system in Schemes 1 and 2 and are utilized once again herein. Notably, a considerable collection of literature exists citing and using the mechanisms in Scheme 3 (over 1240 total citations as of April 2019) to account for a myriad of nucleating, growing, and agglomerating systems across nature. This fact will become important in suggesting the broader generality and importance of ME-PBM and its full Ordinary Differential Equation (ODE) approach developed and utilized in what follows.

Scheme 3 shows the classic FW 2-step[14] (steps 1 and 2), 3-step (steps 1−3), and two 4 pseudoelementary step mechanisms (steps 1−4 or 1−3 and 4′). These are deliberately minimalistic mechanisms for transition metal nanoparticle formation and agglomeration.[14,34−40] Dihydrogen (H_2) is shown below the arrow where it is involved in the reaction. Nucleation is illustrated as unimolecular for simplicity, as it is in the FW 2-step mechanism,[14] and for the sake of illustration of the minimum mechanisms. It should be noted, however, that bimolecular[17] as well as net termolecular nucleation[18] have been demonstrated in recent work.[17,18] A *new* 3-step mechanism has resulted from the present studies, *vide infra*. This new mechanism consists of steps 2−3 added together to become a single step (A + B → C), plus steps 1 and 4′, as will be detailed in an upcoming section of this paper.

Hence, now available for use with the PBM approach are the minimalistic, Ockham's razor-obeying nanoparticle formation mechanisms consisting of 2,[14] 3,[34] and 4 steps.[35−38] Each mechanism is extensively disproof-based; for example, over 21 alternative mechanisms have been ruled out in formulation of the 4-step mechanisms as documented elsewhere.[35−38] The kinetic models in Scheme 3 consist of the following pseudoelementary steps: (i) *slow continuous nucleation*[14] as well as *autocatalytic surface growth* (the FW 2-step mechanism);[14] (ii) two types of agglomeration (bimolecular and autocatalytic agglomeration);[35−38] and (iii) secondary autocatalytic surface growth.[38] Additionally and importantly, a ligated precursor[18,43] and ligated-particle product[43] reversible (equilibria) steps have recently appeared[18,43] that promise to be crucial in accounting for ligand-based particle size and size distribution control. The latter is due to important work from the laboratories of Professor A. Karim and his students.[43] Those additional (pseudoelementary) steps (not shown in Scheme 3) are (iv) A·L ⇌ A + L[18,43] and (v) ligated-particle product B·L ⇌ B + L.[43]

DOI: 10.1021/jacs.9b06364
J. Am. Chem. Soc. 2019, 141, 15827−15839

An important but little recognized point is that such disproof-obtained and deliberately minimalistic pseudoelementary step mechanisms are what one must strive for first in studying the mechanisms of complex multistep reactions such as nanoparticle formation and, for example, Noyes' classic work on oscillating reactions where the pseudoelementary step concept was developed and popularized.[33] Furthermore, the correct pseudoelementary steps are composites of the true underlying elementary steps[14,33] which in favorable cases[44] can then be uncovered and shown to add up to the curve-fit pseudoelementary steps.[44] The telling case history in ref 44 is worth study as an illustration of the power and use of the pseudoelementary step concept in deducing the underlying mechanisms of complex systems. Put another way, pseudoelementary steps and minimalistic mechanisms such as those in Scheme 3 *are required* to eventually get to the more detailed, more atomistic, and ideally closer to correct underlying mechanism(s), as well as for ME-PBM,[45] *vide infra*.

4. EXPERIMENTAL SECTION

4.1. Cyclohexene Reporter Reaction Kinetics. The cyclohexene hydrogenation catalytic reporter reaction (CHCRR) kinetic data (as well as the PSD data, *vide infra*) examined herein by ME-PBM were obtained for the $\{(1,5\text{-COD})Ir^{I}\cdot POM\}^{8-}$ precursor and precatalyst. The well-established, balanced stoichiometry for formation of $Ir(0)_n$ nanoparticles under H_2 leading to $Ir(0)_n$ nanoparticles stabilized by coordinated POM^{9-} polyanions[14,24,25] is shown back in Scheme 1. The kinetics of nanoparticle formation were followed *indirectly*, but continuously and in real-time, by the catalytic reporter reaction method, specifically the CHCRR method illustrated in Scheme 4.[14,34−40] Part I of Scheme 4 displays the FW 2-step mechanism, where A = $\{(1,5\text{-COD})Ir^{I}\cdot POM\}^{8-}$ and B = the $Ir(0)_n$ product, and the CHCRR method for monitoring the formation of $Ir(0)_n$. In Part II, the pseudoelementary step method for monitoring the CHCRR is displayed. The resultant differential relationships from Scheme 4 are expressed in eq 1:

Scheme 4. (I) Illustration of the FW 2-Step Mechanism and the Cyclohexene Hydrogenation Catalytic Reporter Reaction (CHCRR) Method[14,34−40] and (II) Illustration of the Pseudoelementary Step Method for Monitoring the CHCRR

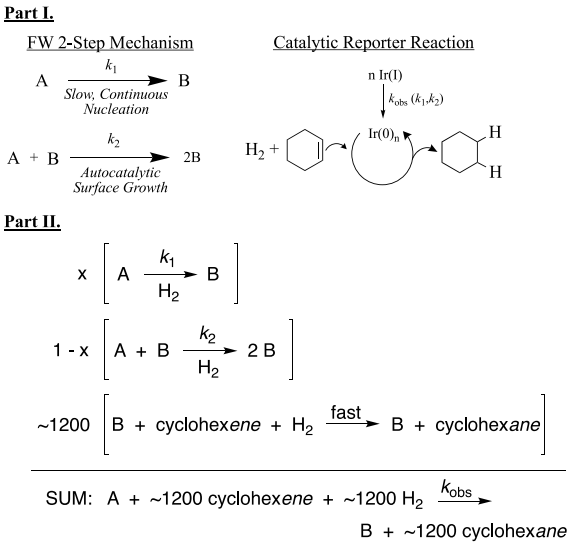

$$\frac{-d[A]}{dt} = \left(\frac{1}{1200}\right)\left(\frac{-d[\text{cyclohexene}]}{dt}\right) = \left(\frac{1}{1200}\right)\left(\frac{-d[H_2]}{dt}\right) = \frac{+d[B]}{dt} \quad (1)$$

The indirect CHCRR kinetic monitoring method relies on having an excess of cyclohexene and H_2 relative to the precursor concentration [A] and on the cyclohexene hydrogenation (rightmost catalytic cycle) being fast compared to the rates of the nucleation (k_1) and autocatalytic growth (k_2) steps shown to the left. The required fast catalytic hydrogenation (and, hence, the general validity of the CHCRR method, at least through the first ca. 1/2 of the curve, *vide infra*) has been confirmed multiple times by demonstrating a zero-order dependence on the initial [cyclohexene] concentration.[14,34−38] The CHCRR has also been checked by following the loss of A = $\{(1,5\text{-COD})Ir^{I}\cdot POM\}^{8-}$ by monitoring the formation of cyclooctane by GLC[14] (see the balanced reaction stoichiometry in Scheme 1). However, as the nanoparticle formation reaction and concomitant catalytic hydrogenation and CHCRR proceed, cyclohexene is consumed, and the zero-order $[\text{cyclohexene}]^0$ condition eventually breaks down. Hence, only the first halves of kinetic curves obtained by the CHCRR are typically used in the curve-fitting.[14,34−38] The ME-PBM herein will turn out to serve as a further check on the CHCRR kinetic methodology and will confirm that only the first half (approximately) of a CHCRR kinetic curve is useful (as has long been known from examining the assumptions and approximations behind the CHCRR methodology).[14] More specifically, we will see that the best fits of the PSDs can actually be used to predict the deviations from the second half of the CHCRR curve.

4.2. Particle-Size Distribution Data. The PSDs for the $\{(1,5\text{-COD})Ir^{I}\cdot POM\}^{8-}$ data were generated from experiments prepared by Finney and from transmission electron microscopy (TEM) micrographs taken at Clemson University.[46] Conditions for the TEM sample preparations were 1.2 mM $\{(1,5\text{-COD})Ir^{I}\cdot POM\}^{8-}$ in acetone.[46] The PSDs were created by measuring and organizing the particle sizes into bins at ±0.05 nm intervals (i.e., 0.1 nm total; 0.85−0.94 nm were considered to be 0.90 nm, 0.95−1.04 were considered to be 1.00 nm, etc.). The four distributions presented *vide infra* were collected at 0.918, 1.170, 2.336, and 4.838 h (the original times were measured in seconds, then converted to hours and the correct number of significant figures indicated), with 246, 61, 150, and 213 particles measured, respectively. The mean sizes and standard deviations are, respectively, 2.0 ± 0.4 nm, 2.4 ± 0.6 nm, 2.5 ± 0.4 nm, and 2.8 ± 0.4 nm. The PSD data are, by design, the same data that an earlier PBM attempted to treat,[32] so the results of the present ME-PBM could be compared to that prior, nonfully mechanism-enabled PBM effort (which led to the aforementioned erroneous conclusion/assertion that continuous nucleation had to be somehow suppressed).[32]

4.3. Measurement of K_{Diss} and k_{1alt}. The K_{Diss} equilibrium constant in Scheme 2 was obtained by ^{31}P NMR for the $\{(1,5\text{-COD})Ir^{I}\cdot POM\}^{8-}$ system, as detailed elsewhere, and originally in propylene carbonate solvent at 22 °C and as $K_{Diss,apparent} = K_{Diss}[\text{Solvent}]^2 = (6.4 \pm 1.4) \times 10^{-5}$ M,[18] where $[\text{Solvent}]^2 = [\text{neat propylene carbonate}]^2 = (12.1\ \text{M})^2$. As a check, $K_{Diss(acetone)} \sim 5 \times 10^{-7}$ M 22 °C was measured by ^{31}P NMR in acetone following the same published methods.[18] Because the two K_{Diss} values are within experimental error, the somewhat more precise $K_{Diss} \approx 3 \times 10^{-7}\ M^{-1}$ value was used in the ME-PBM, along with $[\text{Solvent}]^2 = (11.3\ \text{M})^2$ for acetone under the conditions employed that include the excess cyclohexene for the CHCRR.[47]

The k_{1alt} ($= k_{1,alt.termolecular} = (6.4 \pm 1.6) \times 10^4\ M^{-2}\ h^{-1}$) rate constant in Scheme 2 was determined in a prior report[18] by CHCRR kinetics experiments at a constant concentration of 1.2 mM $\{(1,5\text{-COD})Ir^{I}\cdot POM\}^{8-}$ in propylene carbonate with deliberately added, varied amounts of $[POM^{9-}]_{Added}$ from 0.15−2.1 mM. Deconvolution of that kinetic data to yield k_{1alt} was performed by fitting to the

DOI: 10.1021/jacs.9b06364
J. Am. Chem. Soc. 2019, 141, 15827−15839

alternative termolecular mechanism in Scheme 2, all as previously reported.[18]

4.4. Population Balance Modeling with PSD and CHCRR Curve-Fitting: Resurrecting Smoluchowski's Classic 1918 Full ODE Approach to the PBM. We followed Smoluchowski's classic 1918 article[48,49] in which he created a discrete model (in that case for particle agglomeration) for particle formation. This avoids using ODE approximations to solve the population balance equation (PBE), which is a partial differential equation that assumes particle size to be a continuous variable.[11] Instead, we more simply and more powerfully use the full system of ODEs that corresponds to an approaching-atomistic account of our $Ir(0)_n$ formation system at the discrete kinetic level. An important result of our Smoluchowski-type full ODE PBM which follows is that it allows a rare direct computation of the PSD shape from the ME-PBM as well as *curve-fitting of that predicted shape to the experimental PSD* (i.e., rather than just a visual, "eyeball" comparison of experimental data to moment-based averages). This approach is possible since the data we work with in this paper involves sufficiently small particle sizes (simulated particles consisting of ≤2500 monomers), so the full, derived system of ODEs can be solved numerically in a reasonable amount of computation time (typically <5 min) on a laptop computer.

The ODE system models of the mechanisms that follow were coded in MATLAB. Details of the code beyond what are provided in the main text, including the needed interpretation of the pseudoelementary step mechanisms at the atomistic level, are provided in Figure S3. Due to the inherent stiffness of the problem, MATLAB's *ode15s* function was chosen as the solver. Even using this stiff ODE solver, the relative and absolute tolerances needed to be made substantially smaller than the default values of 10^{-3} and 10^{-6} to avoid unphysical oscillations. Both were chosen to be 10^{-13}, but it was noticed that larger values are possible without the creation of the unphysical oscillations. These small tolerance values increase the computation time, but that time remains under 5 min except in cases where mechanisms include agglomeration (e.g., those which contain step 3 or, especially, step 5 in Scheme 3). Hence, no large effort was needed nor made to optimize computation time by maximizing the tolerances. The simulations were primarily performed on a late 2013 MacBook Pro with a fourth-generation Intel Core i7 processor at 2.3 Ghz and 16 GB 1600 MHz DDR3 RAM. The (shortest) 2-step mechanism takes around 30 s, while the (longest) 4-step alternative termolecular nucleation mechanism takes around 2 min. The code is freely available on github at the following link: https://github.com/drhandwerk/pbm.

Fitting was done using MATLAB and the *patternsearch* algorithm, usually to 150 iterations, unless the algorithm converged earlier. The *patternsearch* algorithm is capable of minimizing a multivariable objective function with constraints. This was helpful to constrain the problem not only to positive, physically relevant rate constants but also to any other known, experimentally determined constants (such as the K_{Diss} in Scheme 2 of the alternative termolecular nucleation mechanism). Fittings were done to either the CHCRR curve or to the histogram at the fourth time of 4.838 h. The objective function for the CHCRR fit uses MATLAB's *norm* function to take the L^2 norm of the difference between the experimental and simulated curves. For the histogram fit, the integral L^1 norm was used as the objective function with the *trapz* function after interpolating the experimental data and the simulated solution to be on the same domain via *griddedInterpolant*. The best function value (BFV) is the last result of the appropriate objective function and is reported in the figure captions, with smaller BFVs indicating better fits. Further information for a given fit is also provided in the appropriate figure caption.

4.5. Disproof-Based Approach to the PBM in the Present Work. All of the ME-PBM work that follows was performed with strict adherence to the preferred scientific method[41,42] of disproof of multiple alternative hypotheses, as was the prior work leading to the minimum mechanisms used to enable the PBM.[14,17,18,35−38] As Platt's classic paper notes, "...for exploring the unknown, there is no faster method."[42] The disproof-based nature of the PBM herein is an important feature of our ME-PBM approach. More specifically, 12 ME-PBMs were considered and 11 ME-PBMs were disproved en route to the best-fitting ME-PBM, enabled by the finding of a new 3-step mechanism that is highlighted in the following text.

5. RESULTS AND DISCUSSION

5.1. Description of the 12 Specific Mechanisms and ME-PBMs Tested. The 12 ME-PBMs built from 12 specific mechanisms using various steps in Scheme 3 were tested. The specific mechanisms that ME-PBMs were constructed from include the following: (i) the 2-step mechanism (steps 1 and 2, Scheme 3); (ii) a 4-step mechanism (steps 1−3 and 4′ in Scheme 3); (iii) the classic 3-step mechanism given in Scheme 3 (i.e., steps 1−3 in Scheme 3); (iv) a second 4-step mechanism (steps 1−4 in Scheme 3); (v) a 5-step mechanism including all of the steps in Scheme 3; and (vi) a new 3-step mechanism that resulted from the PBM analysis, *vide infra*. We tested simple unimolecular, bimolecular, termolecular, and fourth-order nucleation (as a check and control) with many, albeit not all, of the 6 primary mechanisms cited above. In each of the above 6 primary mechanisms the *experimentally determined* alternative termolecular nucleation was tried along with the alternative of simple termolecular nucleation in A (i.e., Ir_3). The best mechanism and associated ME-PBM of the 12 tested to try to fit the experimental PSD is presented in section 5.3.

5.2. Basic FW 2-Step Mechanism. The first mechanism examined is the FW 2-step mechanism shown as the first two steps (steps 1 and 2) in Scheme 3. The pseudoelementary steps consisting of slow, continuous nucleation together with autocatalytic (surface) growth[14] are

$$\begin{aligned} \mathrm{A} &\xrightarrow{k_1} \mathrm{B} \\ \mathrm{A} + \mathrm{B} &\xrightarrow{k_2} 2\mathrm{B} \end{aligned} \tag{2}$$

5.2.1. Derivation of the 2-Step Mechanism-Enabled PBM. First, some required notation: let the concentration (in mol/L) of precursor monomers be denoted by m_1. The concentration of particles of size j, which consist of j monomers, is denoted by n_j. The collection of particles of size j therefore contains a total of jn_j monomers per unit volume. Initially, our differential equations will be written in terms of this total concentration of monomers that are contained in particles of a given size j, denoted by $m_j = jn_j$ (hence, $m_1 = n_1$). The concentration of binding sites on a particle of size j will be known as b_j. The relationship between the total concentration of monomers in particles of size j and the concentration of those that are available to bind is given by the relationship $b_j = r(j)m_j$, where the (dimensionless) function $r(j)$ can represent various effects such as volume- or surface-area-dependent growth[14] or ligand capping.[43] Indeed, if we define a new function $\hat{r}(j) = k_i r(j)$, then this new function represents all growth processes for a particle of size j, and $\hat{r}(j)$ is called *the growth kernel*. In what follows, we keep the rate constants k_i and the function $r(j)$ explicit.

Unlike the PBE which has no direct particle−particle interactions,[32] our model is based on atom-to-atom contact. As such, the monomers on the particle surface should be capable of binding, while those on the inside are unreactive. Therefore, a surface area model is adapted by choosing the function $r(j) = 2.677j^{0.72}/j$. This is the number of surface monomers divided by the total number of monomers where the number of surface atoms is taken from Schmidt and Smirnov,[50] and where the natural number j represents the

DOI: 10.1021/jacs.9b06364
J. Am. Chem. Soc. 2019, 141, 15827−15839

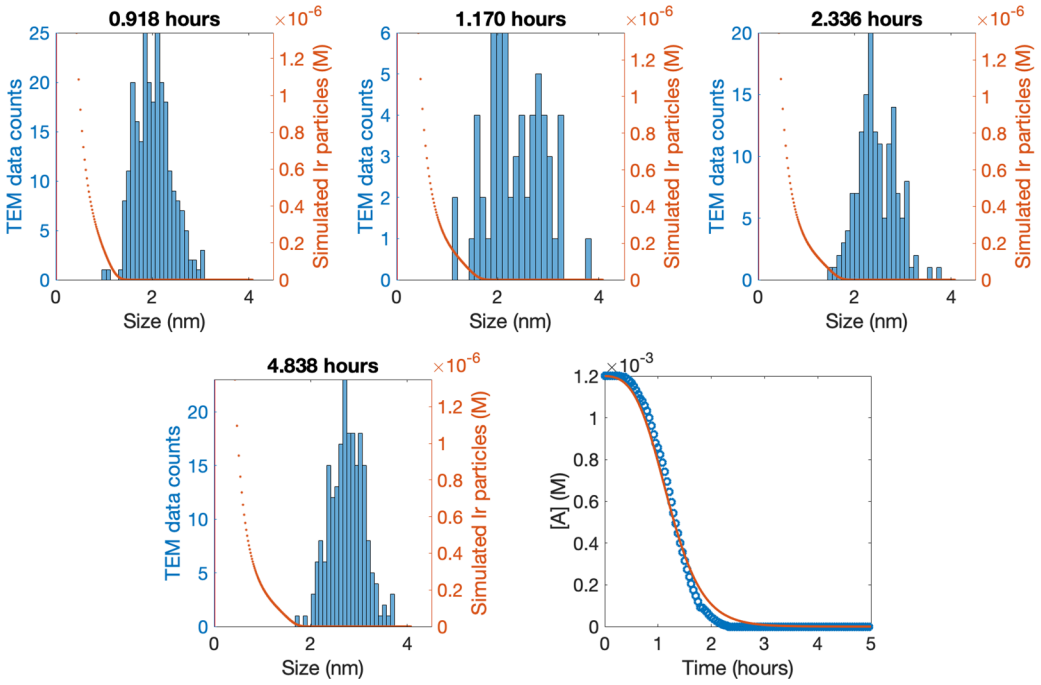

Figure 1. Fit to the CHCRR curve (bottom, far right) using the classic FW 2-step mechanism and first-order nucleation. The rate constants produced by the fit are $k_1 = 6.70 \times 10^{-3}$ h^{-1} and $k_2 = 2.52 \times 10^{3}$ M^{-1} h^{-1}, which are then used to produce the simulations (red dots) that are compared to the four experimental TEM PSDs (blue histograms) shown (top three and bottom left). The BFV is 3.92×10^{-4}. In response to a query from a referee, the right vertical axes for the PSDs and the vertical axis for the reporter reaction should be interpreted as written (e.g., with the top number in the bottom right CHCRR figure being [A] = 1.2×10^{-3} M). This same convention applies for all subsequent figures.

particle size. Note that the $r(j)$ function adapted from the work of Schmidt and Smirnov is just their continuous, hence better, number of surface atoms "scaling factor"[14] than that provided in the 1997 paper first detailing the FW 2-step mechanism.[14]

The following derivation of the 2-step ME-PBM can be generalized to any order of nucleation, including first and second. Let ω be the nucleation order. Using the law of mass action, we obtain the system

$$\frac{dm_1}{dt} = -\omega k_1 m_1^{\omega} - k_2 m_1 \sum_{j=\omega}^{\infty} b_j$$

$$\frac{dm_\omega}{dt} = \omega k_1 m_1^{\omega} - \omega k_2 m_1 b_\omega$$

$$\frac{dm_j}{dt} = j k_2 m_1 (b_{j-1} - b_j) \quad (3)$$

for the change in concentrations of the monomers in particles of all sizes.

Using the above substitutions yields the ODE system

$$\frac{dn_1}{dt} = -\omega k_1 n_1^{\omega} - k_2 n_1 \sum_{j=\omega}^{\infty} r(j) j n_j$$

$$\frac{dn_\omega}{dt} = k_1 n_1^{\omega} - \omega k_2 n_1 r(\omega) n_\omega$$

$$\frac{dn_j}{dt} = k_2 n_1 ((j-1) r(j-1) n_{j-1} - j r(j) n_j) \quad (4)$$

We now have a system for the change in the number of particles of all sizes. Note the similarity between the right-hand side of the n_j equation and the average flux across a "cell" (in PBM language).

The 2-step mechanism with first-order nucleation is capable of closely matching the CHCRR curve when a fit is performed to the CHCRR, as in Figure 1. However, the associated PSDs are terrible to say the least. They are monotonically decreasing functions instead of any kind of match to the experimental shape. There are far too many small particles compared to larger sized particles. This (first-)order nucleation mechanism is incapable of accurately reproducing PSDs that are anything close to the experimental PSD data.

Further evidence for the inability of the classic FW 2-step reaction to account for the PSD comes from *trying* to fit to the 4.838 h histogram (i.e., instead of fitting the CHCRR kinetics data). Significantly, first-order nucleation with a size-independent growth rate is so incapable of producing the correctly shaped PSD that an attempted fit to the 4.838 h histogram yields a fit $k_2 = 0$, meaning that the only particles are the nuclei which then never grow. This produces a PSD which is zero everywhere except for the nucleus size. Since the mechanism apparently cannot move the particles over to where the experimental PSD is, the best fit comes from setting the growth to zero which results in the simulation matching the nonexistent ca. 0.0−2.0 nm particles.

Hence, our ME-PBM results match the finding of Kumar and co-workers[32] concluding that the simple 2-step mechanism, while quite able to account for the CHCRR kinetics, is incapable of reproducing the more information-rich PSD. The previously unanswered, but critical, question becomes, "What is minimally required, mechanistically, to be able to match the observed PSD?".

5.3. Winning ME-PBM: Alternative Termolecular Nucleation Plus a New 3-Step Mechanism. After a detailed examination of the 11 other ME-PBMs examined, the winning ME-PBM from among the 12 mechanisms

DOI: 10.1021/jacs.9b06364
J. Am. Chem. Soc. 2019, 141, 15827−15839

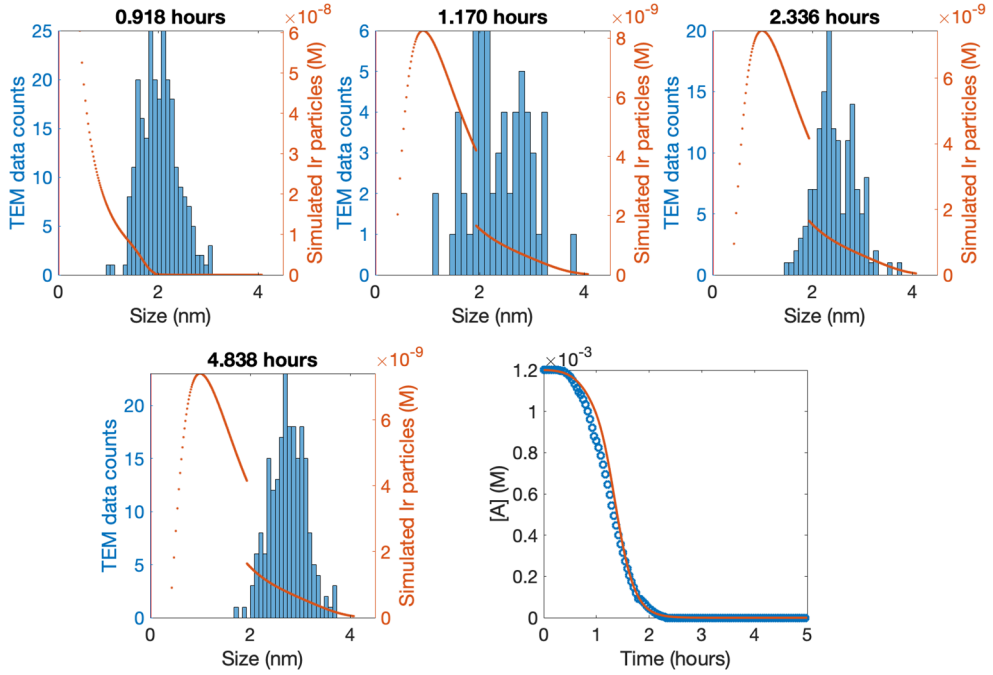

Figure 2. Fit of the CHCRR in the lower right using the new 3-step, alternative termolecular nucleation ME-PBM, while constraining k_{+Diss} = 3.60 × 10^{-2} M^{-2} h^{-1} and k_{-Diss} = 7.27 × 10^{4} M^{-1} h^{-1} as previously mentioned. The resulting parameters are k_1 = 5.58 × 10^{4} M^{-2} h^{-1}, k_2 = 5.04 × 10^{3} M^{-1} h^{-1}, k_3 = 1.27 × 10^{4} M^{-1} h^{-1}, and a B vs C particle-size cutoff M = 268. These were in turn used to generate the simulations shown for the four histograms. The BFV is 9.64 × 10^{-4}.

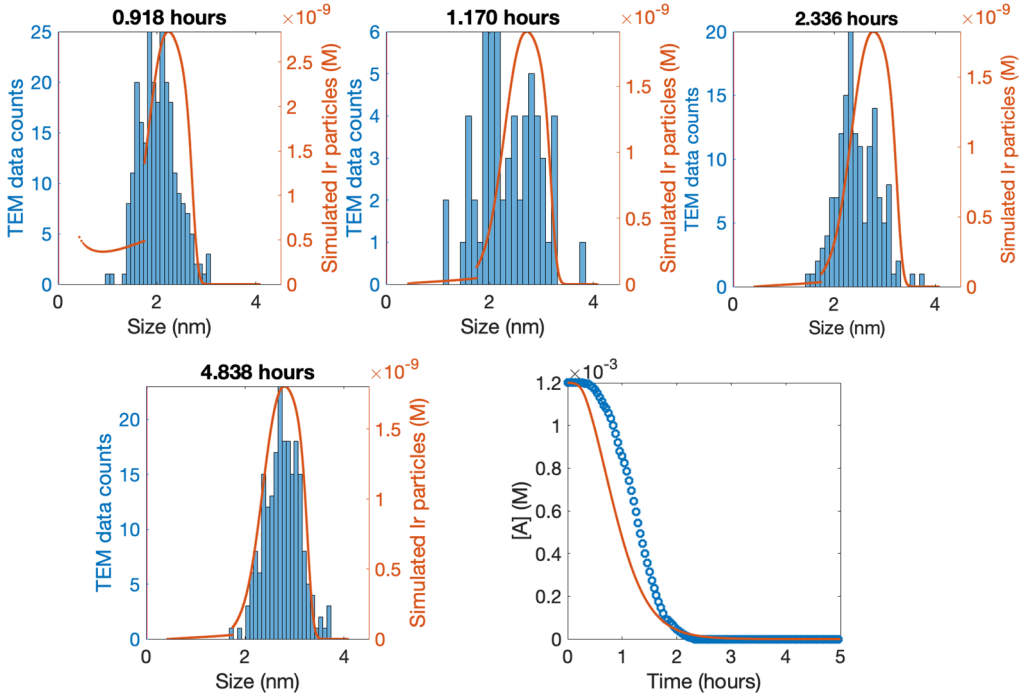

Figure 3. Fit of the final, 4.838 h histogram using the 3-step, alternative termolecular nucleation ME-PBM, with the experimentally established constraints on K_{Diss} (= k_{+Diss}/k_{-Diss}) implemented as previously mentioned as k_{+Diss} = 3.60 × 10^{-2} M^{-2} h^{-1} and k_{-Diss}= 7.27 × 10^{4} M^{-1} h^{-1}, and the k_1 value constrained by its experimentally established upper and lower bounds of (6.4 ± 1.6) × 10^{4} M^{-2} h^{-1}. The resultant fit-determined rate constants are k_1 = 6.50 × 10^{4} M^{-2} h^{-1}, k_2 = 1.60 × 10^{4} M^{-1} h^{-1}, and k_3 = 5.79 × 10^{3} M^{-1} h^{-1} and B vs C particle-size cutoff of M = 197. The computed CHCRR curve using these parameters is shown at the bottom-right. The computed histograms for the first three, earlier time histograms are shown in the top row. The BFV is 23.9 (the BFVs are larger when fitting the PSDs versus when fitting to the reporter reaction due to the use of the L^1 norm for the PSDs and L^2 norm for the reporter reaction).

examined was discovered to be a new 3-step mechanism that is a simple, but critical, 1-step extension of the classic FW 2-step model. The new 3-step mechanism, eq 5 below, is first shown with simple unimolecular nucleation A → B, so the reader can readily understand and visualize this new mechanism compared to the mechanisms in Scheme 3. That said, the

DOI: 10.1021/jacs.9b06364
J. Am. Chem. Soc. 2019, 141, 15827−15839

experimentally correct alternative termolecular nucleation proved to be a key part of the winning ME-PBM that provided the best fits to the PSD data out of all the mechanisms examined (and while still adhering to a minimalistic, Ockham's razor approach). Indeed, using the experimentally correct alternative termolecular nucleation *improved all the ME-PBMs examined*, including over the assumption of simple termolecular nucleation.

The new 3-step mechanism is

$$\begin{aligned} A &\xrightarrow{k_1} B \\ A + B &\xrightarrow{k_2} C \\ A + C &\xrightarrow{k_3} 1.5C \end{aligned} \tag{5}$$

This new mechanism is a 1-step extension of the FW 2-step mechanism. The critical part is that instead of having a constant growth rate for particles of all sizes the *small and large particles are allowed to grow with different rates*. That is, the growth kernel is a step function as implemented in this particular ME-PBM. The evidence that led to this mechanism is that a fitted rate constant tending toward $k_3 \approx 0$ resulted for ME-PBMs examined that included a B + B → C agglomeration step (step 3, Scheme 3) with rate constant k_3. This implies that physical agglomeration is not kinetically important in at least the particular $Ir(0)_n$ formation system examined and under the specific conditions used experimentally. The $k_3 \approx 0$ finding from the ME-PBM (and hence lack of kinetically detectable agglomeration) is pleasingly consistent with and supportive of all of the prior curve-fitting and mechanistic work for the Ir(0) system that led to the original FW 2-step mechanism,[14,24,25] including the use of the indirect but precise data-generating CHCRR kinetic methodology.[14,24,25] Due to the $k_3 \approx 0$ finding, the A + B → 2B and B + B → C steps in Scheme 3 were added to give a single replacement step A + B → C, and in turn, the new 3-step minimum, pseudoelementary step mechanism shown in eq 5 was obtained.

The atomistic interpretation of this mechanism, the appropriate system of ODEs, and how they are implemented in MATLAB, are provided in the Supporting Information. In the implementation of the embedded alternative termolecular nucleation, the known, experimentally determined $K_{Diss} = k_{+Diss}/k_{-Diss}$ in Scheme 2 was constrained to its known value $K_{Diss} = 4.95 \times 10^{-7}$ M^{-1} at 22 °C (implemented via the ratio of $K_{Diss} = k_{+Diss}/k_{-Diss} = (3.60 \times 10^{-2}\ M^{-2}\ h^{-1})/(7.27 \times 10^{4}\ M^{-1}\ h^{-1}) = 4.95 \times 10^{-7}\ M^{-1}$)[47] and k_1 was constrained to its experimentally determined upper and lower bounds $(8.0-4.8) \times 10^{4}\ M^{-2}\ h^{-1}$).[47] In short, this best-performing ME-PBM was implemented using every available piece of experimental information and every piece of available mechanism-enabling data such as the experimentally established nucleation mechanism.

A fit to the CHCRR using the 3-step ME-PBM is given in Figure 2 along with the predicted PSDs formed using the resultant rate constants. The PSDs are poorly fit using the predicted rate constants from fitting the CHCRR. The predicted PSD yields too many small particles.

However, if one instead fits the more *information-rich, final* 4.838 h PSD histogram, the model produces the most accurate size distribution among the 12 total models tested, as seen in Figure 3. The simulation matches well *including the PSD shape* in the 4.838 h histogram; likewise, the earlier three PSDs are pretty well matched. This model is the only simulation of the 12 tried that resulted in a decent fit to the first, early-time PSD histogram. The good fit to the PSD is obtained with just three primary, unconstrained fitting parameters, k_2, k_3 and the small vs large cut-off value, M.

A main physical finding is that in order to obtain the correct shape distribution, the larger particles must grow more slowly than the smaller particles; that is, $k_2 > k_3$. That is the only, but critical, update in the FW 2-step mechanism that is needed to be able to account for the experimentally observed and information-rich, relatively narrow PSD.

The rate constant parameters from fitting the 4.838 h histogram in Figure 3 also resulted in the best match to the CHCRR out of all of the histogram fits (Figure 3, lower right). The reproduction of the CHCRR curve using the PSD-determined rate constants k_1, k_2, and k_3 is not exact, so it remains to be determined where the discrepancy originates from (although as noted earlier, some disagreement is expected given that the conditions and assumptions underlying the CHCRR are known to fail once the concentrations of cyclohexene and dissolved H_2 fall in especially the latter half of the CHCRR curve).[14,34−38] The needed studies are in progress using a second-generation $Ir(0)_n$ nanoparticle precursor $(Bu_4N)_2[(1,5\text{-COD})Ir{\cdot}HPO_4]_2$ system,[31] one where SAXS, XAFS, and GLC and ^1H NMR monitoring of the loss of precursor are all possible in addition to use of the CHCRR as well as TEM-determination of the PSD versus time. Those largely in-hand results are being readied for publication and will be reported in due course. The more general point here is that experimental methods to reliably monitor nanoparticle formation reactions, especially multiple methods that allow rare determinations of the nucleation mechanism(s) and allow better deconvolution of (correlated) nucleation and growth rate constants, continue to be a limiting factor in nanoparticle science across nature. Put another way, this is yet another reason why use of the kinetics information in the PSDs via ME-PBM promises to be quite important in the refinement of nanoparticle formation and subsequent agglomeration mechanisms.

5.3.1. Concept of Mechanism-Enabled Population Balance Modeling. Returning to the general concept of ME-PBM as introduced herein, further powerful if not compelling support for the concept of ME-PBM that is a central theme of the present contribution comes from a look back at the one prior attempt to use PBM with the 2-step mechanism (via a method of moments (MoMs) approximation to solving the PBM equation).[32] That study, which examined the same Ir(0) nanoparticle system and $Ir(0)_n$ formation data utilized herein, did not use the correct (alternative termolecular) nucleation mechanism to mechanistically enable the (ME)-PBM. It instead tried to use inapplicable[14,17,18] CNT and thereby reached a predicted (see footnotes 72 and 75 elsewhere)[17,18] erroneous conclusion that there must be a "... delayed onset of nucleation" (basically a delay somehow in the k_1 step in Scheme 3) "...and its suppression soon after..."[32] (basically then a subsequent suppression of k_1 in Scheme 3), rather deceiving conclusions that are literally the opposite of the critical finding in the present, ***ME***-PBM work. Instead and in dramatic contradistinction, nucleation is *continuous* as demonstrated in 1997.[14] It is differential growth (i.e., faster growth by smaller and slower growth by larger particles) that is what can lead to narrow PSDs despite the inherent PSD broadening effect of continuous nucleation. Given that the cited incorrect conclusion was reached by a high-level expert in PBM, the

DOI: 10.1021/jacs.9b06364
J. Am. Chem. Soc. 2019, 141, 15827−15839

inescapable insight here is clear: *Only true mechanism-enabling* of one's PBM, *plus* a highly disproof-based scientific method as part of PBM,[41,42] holds hope of leading one to correct, reliable PBM-derived conclusions and associated mechanisms. Only by starting out with the correct, *experimentally determined* (alternative termolecular) nucleation mechanism[18] were we led by our ME-PBM analysis to the critical "smaller grow faster than larger" insight.

5.3.2. Important, Noteworthy, and Relevant Literature. Finally, it is important to tie the present work into some other, noteworthy, relevant broader literature. First, a "Mathematical Model for Crystal Growth by Aggregation of Precursor Metastable Nanoparticles" has appeared,[51] which in their assumed mechanism I, is different from (but quite interesting in comparison to) the new 3-step mechanism herein, results that support both studies and hint at the greater generality of the ME-PBM approach developed herein and its resultant new 3-step mechanism. A follow-up paper from those authors in 2006 is also noteworthy.[52] Second, polymer chemists have addressed polymer product distribution problems that are different than the PSD problem addressed herein but that are of considerable interest and hence recommended reading.[53−55] Third, ligand effects[43,56] are very likely one underlying, physical component of the critical finding of "smaller nanoparticles grow faster than larger nanoparticles". The studies of ligand effects on Pd_n particle formation by Karim's group, especially their compelling evidence for a ligated-particle product B·L ⇌ B + L, pseudoelementary step in their informative $Pd_n/POct_3$ system,[43] are especially noteworthy in this regard. Additionally, recent evidence for a slowing of k_{2obs} with added POM^{9-} ligand[56] (i.e., in a FW 2-step analysis of that kinetics data) provides direct kinetics evidence for a ligand effect on growth in the identical $\{(1,5\text{-COD})Ir^{I}\cdot POM\}^{8-}$ precursor and resultant $Ir(0)_n$ nanoparticle system examined in the present ME-PBM contribution.

6. SUMMARY AND CONCLUSIONS

The following is a summary of and the primary conclusions of the present work.

The concept of *Mechanism-Enabled* PBM was introduced, specifically, the notion of enabling one's PBM, regardless of where it occurs across nature, with the experimentally determined nucleation mechanism and then with experimentally determined growth or agglomeration mechanisms. By *mechanism*, we mean what *mechanism* has always meant in classical physical-organic chemistry where it was developed: an Ockham's razor-obeying (therefore deliberately and necessarily minimalistic), disproof-based (and hence as rigorous as possible), and, as needed, pseudoelementary step-based, experimentally determined reaction mechanism well-supported, at a minimum, by a balanced reaction and experimental kinetics studies.

The ME-PBM was implemented via a full ODE approach. The full ODE approach is little used since its 1918 origins,[48,49] but is a powerful approach that allows direct computation of the PSD, *including its* <u>shape</u>, and curve-fitting of the experimental PSD.

Experimentally knowing and inputting the experimentally determined nucleation mechanism proved critical to obtaining reliable results, that is, to *correctly mechanistically enable* the PBM. First, the knowledge of the precise, molecular nucleation mechanism enormously simplified the number of PBMs that had to be considered; only those nucleations of molecularity ≤ 3[17,18] needed to be tested by ME-PBM (although, as a control, nucleation with a molecularity of 4 was also examined herein and proved inferior). The experimentally established, alternative termolecular nucleation[18] for the prototype $Ir(0)_n$ nanoparticle formation system (i) improved the simulated PSDs *in all of the histogram fits* tried, and (ii) overall provided the best fits to both the PSDs and to the CHCRR kinetics data. Those results in turn provide considerable support for and confidence in the prior work leading to the alternative termolecular nucleation mechanism,[18] the CHCRR kinetics methodology[14] employed to discover that nucleation mechanism,[18] and the resultant ME-PBM herein employing the alternative termolecular nucleation mechanism.

A previously unknown 3-step mechanism was discovered that is a simple, but critical, 1-step extension of the FW 2-step mechanism. This discovery is an example of the power of ME-PBM to offer one solution to the "inverse problem" in at least the present example.

The newly discovered 3-step ME-PBM teaches that past knowing the correct nucleation mechanism *particle growth is fundamentally monomer addition* at least under conditions where agglomeration is not kinetically competitive as is the case for the present $Ir(0)_n$ formation. The knowledge that particle growth is fundamentally monomer addition, in at least the present example, in turn yields the best evidence to date that the A+ B→ 2B autocatalytic pseudoelementary step of the FW 2-step mechanism represents the summation of the individual $A + B_j \rightarrow B_{j+1}$ monomer addition steps. This is physically as expected but previously was not experimentally strongly supported. The evidence that particle growth is fundamentally monomer addition also reinforces the use of a full ODE approach to the PBM whenever possible, as the full ODE takes into account the monomer addition steps possible in the ME-PBM under consideration.

The evidence is now compelling that the classic FW 2-step mechanism and the new 3-step minimum mechanisms with their <u>continuous nucleation</u>,[14] the opposite of the now disfavored[15] LaMer assumption[16] of "instantaneous nucleation", constitute *a major paradigm shift* in the understanding of particle formation in the now 69 years since the LaMer model was first introduced in 1950.[16] The literature application of the FW 2-step mechanism, and by implication now the refined new 3-step mechanism, is across a wide variety of systems in nature ranging from homogeneous catalyst formation,[44,57,58] heterogeneous catalyst formation,[59−61] protein aggregation,[62−65] solid-state kinetics,[66,67] dye aggregation,[68] and other areas of nature showing "cooperative", autocatalytic phenomena.[69] The FW 2-step mechanism and the new 3-step mechanism provide slow, continuous nucleation and autocatalytic surface growth to replace both CNT[15,17] (i.e., that is inapplicable to strong-bonded systems)[15,17] and to replace the often cited assumption of "instantaneous" nucleation followed by "diffusion-controlled" growth based on the LaMer model.

The second, seminal finding and associated paradigm shift in the understanding of particle formation, which is supported by all our ME-PBM efforts herein, answers the previously perplexing question of "How can narrow particle-size distributions result in the absence of the inapplicability of CNT to strong-bonded systems[14,17,18,31] and the inapplicability of LaMer's model of "burst" nucleation?".[15] *The paradigm-shifting insight* is that narrow size distributions can and do result when *smaller particles grow faster than larger ones*, i.e., $k_2 > k_3$, when using the 3-step mechanism. This allows the smaller

DOI: 10.1021/jacs.9b06364
J. Am. Chem. Soc. 2019, 141, 15827−15839

particles from continuous nucleation[14] to catch up in size with the more slowly growing larger particles, leading to *surprisingly narrow, near-monodisperse PSDs*. This "smaller grow faster than larger" particles concept replaces the need for repeated claims without evidence of "burst nucleation",[16] and explains how the size broadening effects of continuous nucleation is overcome by smaller particles growing faster than larger ones to yield narrow PSDs.[14]

7. ANTICIPATED IMPACT AND CAVEATS

One can anticipate a broader, more general application and impact of the ME-PBM and the full ODE and PSD-shape-fitting methods herein.[70] The evidence supporting this statement is as follows: (a) The underlying, deliberately minimalistic particle formation mechanisms are more general and already widely cited (≥1240 total citations as of April 2019). (b) Population Balance Modeling is in principle general and hence extendable to systems in nature as varied as "the size and age distribution of fish in a lake, spatial distribution of cars on a freeway, activity and area distribution of particles in a catalysis bed, molecular distribution of polymer in a reactor, and size distribution of droplets in an emulsion,"[8] among many, many other countable entities that form as distributions across nature. Additionally, a broader application of ME-PBM can be anticipated (c) because the full ODE approach we have employed for the PBM problem, and which allows fitting of the PSD and its shape, is extendable and general depending upon the computational power available, while noting that a limitation of the full ODE approach is that the number of computational steps grows steeply with the size of the particle, especially if agglomeration steps need to be included in the mechanisms tested. Other caveats and limitations of ME-PBM and the full ODE approach exist and are worth noting, as summarized below and as will be presented in a full version of our ME-PBM studies.[71] Additionally, the underlying physical reason(s) behind the "smaller particles grow faster than larger particles" finding remain(s) to be elucidated, ligand effects[43,55] having precedent as at least part of the probable answer. However, the results herein, as well as the literature of PBM,[8−13] strongly suggest that henceforth no mechanism of particle formation should be published without testing of and input from the information-rich PSD via ***ME***-PBM. Additionally and most importantly, a new paradigm has been uncovered for how narrow PSDs can be achieved despite continuous nucleation[14] (and in the absence of evidence for burst nucleation[15]), namely, the concept that "smaller particles grow faster than larger particles" and thereby catch up in size with those larger, final particles.

■ ASSOCIATED CONTENT

Supporting Information

The Supporting Information is available free of charge on the ACS Publications website at DOI: 10.1021/jacs.9b06364.

Simulations and PSD curve-fitting; atomistic interpretation of mechanisms; ODEs for the new 3-step mechanism (PDF)

■ AUTHOR INFORMATION

Corresponding Authors

*E-mail: shipman@math.colostate.edu (P.D.S.).
*E-mail: Richard.Finke@colostate.edu (R.G.F.).

ORCID

Derek R. Handwerk: 0000-0003-4614-9954
Patrick D. Shipman: 0000-0003-4741-9370
Saim Özkar: 0000-0002-6302-1429
Richard G. Finke: 0000-0002-3668-7903

Notes

The authors declare no competing financial interest.

■ ACKNOWLEDGMENTS

This work was supported by Colorado State University, revised by the U.S. Department of Energy (DOE), Office of Science, Office of Basic Energy Sciences, Division of Chemical Sciences, Geosciences & Biosciences, via DOE grant SE-FG402-02ER15453 as well as the National Science Foundation Division of Mathematical Sciences, via NSF grant DMS-1814941. Professor Phil Schneider at Murdock University in Australia is thanked for sharing his knowledge of PBModeling and the plus/minus aspects of the Method of Moments in the early stages of this work. Professor A. Karim and his group at Virginia Tech are also thanked for their input and helpful discussions, especially for sharing their own PBM efforts and conclusions with their important Pd/$POct_3$ nanoparticle system[43] as well as for an ongoing collaboration.

■ REFERENCES

(1) Che, M.; Bennett, C. O. The Influence of Particle Size on the Catalytic Properties of Supported Metals. *Adv. Catal.* **1989**, *36*, 55−172.
(2) van Hardeveld, R.; Hartog, F. Influence of Metal Particle Size on Nickel-on-Aerosil Catalysts on Surface Site Distribution, Catalytic Activity, and Selectivity. *Adv. Catal.* **1972**, *22*, 75−113.
(3) Libert, S.; Goia, D. V.; Matijević, E. Internally Composite Uniform Colloidal Cadmium Sulfide Spheres. *Langmuir* **2003**, *19*, 10673−10678.
(4) Hendricks, M. P.; Cossairt, B. M.; Owen, J. S. The Importance of Nanocrystal Precursor Conversion Kinetics: Mechanism of the Reaction between Cadmium Carboxylate and Cadmium Bis-(diphenyldithiophosphinate). *ACS Nano* **2012**, *6*, 10054−10062.
(5) Li, Y.; Pu, C.; Peng, X. Surface activation of colloidal indium phosphide nanocrystals. *Nano Res.* **2017**, *10*, 941−958.
(6) Abécassis, B.; Bouet, C.; Garnero, C.; Constantin, D.; Lequeux, N.; Ithurria, S.; Dubertret, B.; Pauw, B. R.; Pontoni, D. Real-Time in Situ Probing of High-Temperature Quantum Dots Solution Synthesis. *Nano Lett.* **2015**, *15*, 2620−2626.
(7) Libert, S.; Gorshkov, V.; Goia, D. V.; Matijević, E.; Privman, V. Model of Controlled Synthesis of Uniform Colloid Particles: Cadmium Sulfide. *Langmuir* **2003**, *19*, 10679−10683.
(8) Randolph, A. D. A population balance for countable entities. *Can. J. Chem. Eng.* **1964**, *42*, 280−281.
(9) Hulburt, H. M.; Katz, S. A statistical mechanical formulation. *Chem. Eng. Sci.* **1964**, *19*, 555−574.
(10) Randolph, A. D.; Larson, M. A. The Population Balance. In *Theory of Particulate Processes. Analysis and Techniques of Continuous Crystallization*; Academic Press: New York, 1971.
(11) Ramkrishna, D. Population Balances. In *Theory and Application to Particulate Systems in Engineering*; Academic Press: New York, 2000.
(12) Ramkrishna, D.; Mahoney, A. W Population balance modeling. Promise for the future. *Chem. Eng. Sci.* **2002**, *57*, 595−606.
(13) Ramkrishna, D. The Status of Population Balances. *Rev. Chem. Eng.* **1985**, *3*, 49−95.
(14) Watzky, M. A.; Finke, R. G. Transition Metal Nanocluster Formation Kinetic and Mechanistic Studies. A New Mechanism When Hydrogen is the Reductant: Slow, Continuous Nucleation and Fast Autocatalytic Surface Growth. *J. Am. Chem. Soc.* **1997**, *119*, 10382−10400.

DOI: 10.1021/jacs.9b06364
J. Am. Chem. Soc. 2019, 141, 15827−15839

(15) Whitehead, C. B.; Özkar, S.; Finke, R. G. LaMer's 1950 Model for Particle Formation of Instantaneous Nucleation and Diffusion-Controlled Growth: A Historical Look at the Model's Origins, Assumptions, Equations and Underlying Sulfur Sol Formation Kinetics Data. *Chem. Mater.* **2019**, *317116*.
(16) LaMer, V. K.; Dinegar, R. H. Theory, Production and Mechanism of Formation of Monodispersed Hydrosols. *J. Am. Chem. Soc.* **1950**, *72*, 4847−4854.
(17) Laxson, W. W.; Finke, R. G. Nucleation is Second Order: An Apparent Kinetically Effective Nucleus of Two for $Ir(0)_n$ Nanoparticle Formation From $[(1,5\text{-COD})Ir^{I}\cdot P_2W_{15}Nb_3O_{62}]^{8-}$ Plus Hydrogen. *J. Am. Chem. Soc.* **2014**, *136*, 17601−17615. Please also see the references provided therein.
(18) Özkar, S.; Finke, R. G. Nanoparticle Nucleation Is Termolecular in Metal and Involves Hydrogen: Evidence for a Kinetically Effective Nucleus of Three $\{Ir_3H_{2x}\cdot P_2W_{15}Nb_3O_{62}\}^{6-}$ in $Ir(0)_n$ Nanoparticle Formation From $[(1,5\text{-COD})Ir^{I}\cdot P_2W_{15}Nb_3O_{62}]^{8-}$ Plus Dihydrogen. *J. Am. Chem. Soc.* **2017**, *139*, 5444−5457. Please also see the references provided therein.
(19) Volmer, M.; Weber, A. Z. Keimbildung in übersättigten Gebilden. *Z. Phys. Chem.* **1926**, *119U*, 277−301.
(20) Tohmfor, G.; Volmer, M. Die Keimbildungunter dem Einfluß elektrischer Ladungen. *Ann. Phys.* **1938**, *425*, 109−131.
(21) Volmer, M. *Kinetik der Phasenbildung*; Verlag von Theodor Steinkopff: Leipzig, 1939.
(22) Becker, R.; Döring, W. Kinetische Behandlung der Keimbildung in übersaettigten Daepfern. *Ann. Phys.* **1935**, *416*, 719−752.
(23) Kashchiev, D. *Nucleation: Basic Theory with Applications*; Butterworth Heinemann: Oxford, U.K., 2000.
(24) Lin, Y.; Finke, R. G. Novel Polyoxoanion and Bu_4N^+ Stabilized, Isolable, and Redissolvable, 20−30 Å $Ir_{\sim 300-900}$ Nanoclusters: The Kinetically Controlled Synthesis, Characterization, and Mechanism of Formation of Organic Solvent-Soluble, Reproducible Size, and Reproducible Catalytic Activity Metal Nanoclusters. *J. Am. Chem. Soc.* **1994**, *116*, 8335−8353.
(25) Lin, Y.; Finke, R. G. A More General Approach to Distinguishing "Homogeneous" from "Heterogeneous" Catalysis: Discovery of Polyoxoanion- and Bu_4N^+-Stabilized, Isolable and Redissolvable, High Reactivity $Ir_{\sim 190-450}$ Nanocluster Catalysts. *Inorg. Chem.* **1994**, *33*, 4891−4910.
(26) Oxtoby, D. W. Homogeneous Nucleation: Theory and Experiment. *J. Phys.: Condens. Matter* **1992**, *4*, 7627−7650.
(27) Zhang, T. H.; Liu, X. Y. Nucleation: What Happens at the Initial Stage? *Angew. Chem., Int. Ed.* **2009**, *48*, 1308−1312.
(28) Note the "Two-Step Model" referred to in the following work and associated literature, involving an amorphous, pre-nucleation, dense phase, and/or clusters, is distinct from and should not be confused with the FW 2-step mechanism[14] of continuous nucleation and autocatalytic surface growth: Erdemir, D.; Lee, A. Y.; Myerson, A. S. Nucleation for Crystals from Solution: Classical and Two-Step Models. *Acc. Chem. Res.* **2009**, *42*, 621−629.
(29) Nucleation−A Transition State to the Directed Assembly of Materials, *Faraday Discussions*; Faraday Discussions Series, Royal Society Of Chemistry: U.K., 2015, *179*, 9−154.
(30) The "strongly associated" systems in the following review correspond in a general way to what we denote as "strongly bonded" systems in the present research: Zhang, R.; Khalizov, A.; Wang, L.; Hu, M.; Xu, W. Nucleation and Growth of Nanoparticles in the Atmosphere. *Chem. Rev.* **2012**, *112*, 1957−2011.
(31) Whitehead, C. B.; Finke, R. G. Nucleation Kinetics and Molecular Mechanism in Transition-Metal Nanoparticle Formation: The Intriguing, Informative Case of a Bimetallic Precursor, $\{[(1,5\text{-COD})Ir^{I}\cdot HPO_4]_2\}^{2-}$. *Chem. Mater.* **2019**, *31*, 2848−2862. Please also see the references provided therein.
(32) Perala, S. R. K.; Kumar, S. On the Two-Step Mechanism for Synthesis of Transition-metal Nanoparticles. *Langmuir* **2014**, *30*, 12703−12711.
(33) Field, R. J.; Noyes, R. M. Oscillations in chemical systems. 18. Mechanisms of chemical oscillators: conceptual bases. *Acc. Chem. Res.* **1977**, *10*, 214−221. Please also see the references provided therein. As we first noted in footnote 31 elsewhere,[17] "The concept of pseudoelementary steps was introduced in the 1970s by Noyes, who developed this concept using kinetic studies of complex oscillating reactions. By pseudo-elementary we mean collections of one or more slow steps, plus any number of faster steps, that when added together yield a balanced reaction that can be uses as effectively elementary (i.e., as pseudo-elementary) for the purposes of kinetic treatments in the same way that truly elementary steps are used as the basic building blocks of reliable reaction mechanisms. That said, the reaction order of a pseudo-elementary step cannot be directly used to imply the molecularity of that (composite) step as is the case with a true elementary step."
(34) Hornstein, B. J.; Finke, R. G. Transition-Metal Nanocluster Kinetic and Mechanistic Studies Emphasizing Nanocluster Agglomeration: Demonstration of a Kinetic Method That Allows Monitoring All Three Phases of Nanocluster Formation and Aging. *Chem. Mater.* **2004**, *16*, 139−150; see also the addition/correction: *Chem. Mater.* **2004**, *16*, 3972.
(35) Besson, C.; Finney, E. E.; Finke, R. G. A Mechanism for Transition-Metal Nanoparticle Self-Assembly. *J. Am. Chem. Soc.* **2005**, *127*, 8179−8184.
(36) Besson, C.; Finney, E. E.; Finke, R. G. Nanocluster Nucleation, Growth and Then Agglomeration Kinetic and Mechanistic Studies: A More General, Four-Step Mechanism Involving Double Autocatalysis. *Chem. Mater.* **2005**, *17*, 4925−4938.
(37) Finney, E. E.; Finke, R. G. The Four-Step, Double-Autocatalytic Mechanism for Transition-Metal Nanocluster Nucleation, Growth and Then Agglomeration: Metal, Ligand, Concentration, Temperature, and Solvent Dependency Studies. *Chem. Mater.* **2008**, *20*, 1956−1970.
(38) Kent, P. D.; Mondloch, J. E.; Finke, R. G. A Four-Step Mechanism for the Formation of Supported-Nanoparticle Heterogeneous Catalysts in Contact with Solution: The Conversion of $Ir(1,5\text{-COD})Cl/\gamma\text{-}Al_2O_3$ to $Ir(0)_{\sim 170}/\gamma\text{-}Al_2O_3$. *J. Am. Chem. Soc.* **2014**, *136*, 1930−1941.
(39) Finney, E. E.; Finke, R. G. Nanocluster nucleation and growth kinetic and mechanistic studies: A review emphasizing transition-metal nanoclusters. *J. Colloid Interface Sci.* **2008**, *317*, 351−374.
(40) Özkar, S.; Finke, R. Dust Effects On Nucleation Kinetics and Nanoparticle Product Size Distributions: The Illustrative Case Study of a Prototype $Ir(0)_n$ Transition-Metal Nanoparticle Formation System. *Langmuir* **2017**, *33*, 6550−6562. See also the references in this paper to the history and prior key literature on the effects of dust on particle formation and nucleation kinetics.
(41) Chamberlin, T. C. Studies for Students. The Method of Multiple Working Hypotheses. *J. Geol.* **1897**, *5*, 837−848.
(42) Platt, J. R. Strong Inference. *Science* **1964**, *146*, 347−353.
(43) Mozaffari, S.; Li, W.; Thompson, C.; Ivanov, S.; Seifert, S.; Lee, B.; Kovarik, L.; Karim, A. M. Colloidal nanoparticle size control: experimental and kinetic modeling investigation of the ligand-metal binding role in controlling the nucleation and growth kinetics. *Nanoscale* **2017**, *9*, 13772−13785.
(44) Smith, S. E.; Sasaki, J. M.; Bergman, R. G.; Mondloch, J. E.; Finke, R. G. Platinum-Catalyzed Phenyl and Methyl Group Transfer from Tin to Iridium: Evidence for an Autocatalytic Reaction Pathway with an Unusual Preference for Methyl Transfer. *J. Am. Chem. Soc.* **2008**, *130*, 1839−1841. See the accompanying Supporting Information for the details of how the true elementary steps were deduced, and how they add up to the pseudo-elementary steps that proved necessary, and were used first, to uncover the underlying, elementary-step mechanism, one supported in this case by direct monitoring of all observable species in the catalytic cycle.
(45) Of interest is that ME-PBM as defined and developed herein was at least not probable, and arguably not possible, until now for four reasons: (i) CNT had not been compellingly disproved for strong-bonding systems.[14,17,18,31] It was not previously understood that CNT *cannot* in general be used to enable PBM of at least strong-bonding systems, and if used, will lead to erroneous conclusions (e.g., the

DOI: 10.1021/jacs.9b06364
J. Am. Chem. Soc. 2019, 141, 15827−15839

erroneous conclusion that continuous nucleation must somehow be suppressed in order to achieve narrow size distributions).[32] (ii) The overwhelming evidence disfavoring[15] the 1950 LaMer growth model and its assumed "instantaneous" ("burst") nucleation had not been critically reviewed. Hence, it was not well-known until 2019[15] that the LaMer model *cannot* be used to enable reliable PBM, a critical point and insight given the importance of knowing the nucleation mechanism so as to start the PBM out correctly. (iii) Hence, the crucial molecular mechanism of *nucleation* for a prototype system that could be used in ME-PBM did not exist until 2017.[18] Finally, (iv) it was not widely appreciated that the needed minimum mechanisms for the growth and agglomeration steps do now exist, as shown in Scheme 3, and hence can be used along with an experimentally known nucleation mechanism to properly enable PBM.

(46) Watzky, M. A.; Finney, E. E.; Finke, R. G. Transition-Metal Nanocluster Size vs Formation Time and the Catalytically Effective Nucleus Number: A Mechanism-Based Treatment. *J. Am. Chem. Soc.* **2008**, *130*, 11959−11969.

(47) As detailed in the Experimental section, an estimate of $K_{Diss,\ apparent} = K_{Diss}[Solvent]^2 = (6.4 \pm 1.4) \times 10^{-5}$ M at 22 °C was measured by ^{31}P NMR, originally in propylene carbonate[18] (where $[Solvent]^2 = (12.1\ M)^2$ for neat propylene carbonate). This in turn yields $K_{Diss} = (3.4 \pm 0.8) \times 10^{-7}\ M^{-1}$ in neat, 13.6 M acetone if one assumes that the $K_{Diss,apparent} = K_{Diss}[Solvent]^2$ values should be roughly comparable in these two solvents, an assumption that should be more than adequate for the purposes of the present studies. Moreover, as an experimental check on this assumption, $K_{Diss(acetone)}$ of $\sim 5 \times 10^{-7}$ M 22 C was measured by ^{31}P NMR in acetone following the published methods.[18] Because the two K_{Diss} values are within experimental error as anticipated, the somewhat more precise $K_{Diss} > 3 \times 10^{-7}\ M^{-1}$ value was used in the ME-PBM, along with $[Solvent]^2 = (11.3\ M)^2$ for 2.5 mL of propylene carbonate and 0.5 mL of cyclohexene.

(48) Smoluchowski, M. Versuch einer mathematischen Theorie der Koagulationskinetik kolloider Lösungen. *Z. Phys. Chem.* **1918**, *92U*, 129−168.

(49) The following review provides a summary in English of Smoluchowski's 1918 paper: Chandrasekhar, S. Stochastic Problems in Physics and Astronomy. *Rev. Mod. Phys.* **1943**, *15*, 1−89.

(50) Schmidt, A. F.; Smirnov, V. V. Concept of "magic" number clusters as a new approach to the interpretation of unusual kinetics of the Heck reaction with aryl bromides. *Top. Catal.* **2005**, *32*, 71−75. Note that the surface-atom approximation given by Schmidt and Smirnov has more surface atoms than total atoms for particles smaller than 34. Using this approximation verbatim makes the function r not directly correspond to a percentage of total atoms that are bindable, at least for small sizes, which in turn would have the effect of making smaller sized atoms more reactive than a strictly surface area dependent growth model. The piecewise function $r = \begin{cases} 1, j < 34 \\ s(j), j \geq 34 \end{cases}$ where j is the particle size and $s(j)$ is the Schmidt and Smirnov approximation that is a modification that does not have this deficiency.

(51) The following 2005 paper is a noteworthy contribution, especially for its earlier date (by 14 years), perhaps being the best prior attempt at what we denote herein as ME-PBM. The authors preferred their more complex, 4-step Mechanism II (that has a typo in the second step; it should be $B \rightarrow C_1$, and not the repetitive $B + C_i$ (C_{i+1}). The importance of this paper 2005 paper so noted, key advances reported in our present, 2019, paper critical to true ME-PBM include: the input of disproof-based, experimentally determined nucleation and growth mechanism; quantitative fitting of the PSD; and the key finding of a particle-size-dependent growth. Drews, T. O.; Katsoulakis, M. A.; Tsapatsis, M. Mathematical Model for Crystal Growth by Aggregation of Precursor Metastable Nanoparticles. *J. Phys. Chem. B* **2005**, *109*, 23879−23887.

(52) The following valuable paper reports a prolonged nucleation stage for the zeolite crystal growth with gradual loss of precursor. The nucleation mechanism is not known (is assumed to be first-order and reversible), nor is the primary growth mechanism known (a second step of reversible bimolecular agglomeration of B + B to C is assumed), so while quite interesting, this work does not qualify as ME-PBM by the definition given in the present, 2019, ME-PBM paper. Additionally, the authors assume a constant growth rate for all particle sizes, another critical difference from the 3-step mechanism in the present work. Relevant here is that a 2-step mechanism with its two irreversible steps and two (k_1 and k_2) rate-constant parameters has been shown to fit the Figure 6 zeolite yield versus time data better (see Figure S5 of the Supporting Information of a 2009 paper)[66] than does the 4-parameter model employed in the 2006 paper.[52] Nevertheless, the most important point here is that both the 2006[52] and the prior 2005 studies[51] are valuable earlier studies on the edge of being ME-PBM: Davis, T. M.; Drews, T. O.; Ramanan, H.; He, C.; Dong, J.; Schnablegger, H.; Katsoulakis, M. A.; Kokkoli, E.; McCormick, A. V.; Penn, R. L.; Tsapatsis, M. Mechanistic principles of nanoparticle evolution to zeolite crystals. *Nat. Mater.* **2006**, *5*, 400−408.

(53) Close inspection reveals that the underlying mechanisms and hence accompanying ODEs of initiation and polymerization are not unexpectedly *different* than those for particle formation. The differences arise in no small part due to the monomer and initiator in polymerization reactions *being supplied in known concentrations* versus "monomer" or actually bimetallic[17] or termolecular[18] precursors *being generated* as part of nucleation, growth, and agglomeration in particle formation reactions. Another difference between polymerizations and particle formations is that in a polymerization there is typically just one site from which the polymer grows, while growth in a nanoparticle is possible across multiple surface sites and is surface-ligand-dependent.[43] These differences so noted, the two cited excellent, relevant contributions from the polymer distributions literature are recommended reading.[53,54] We thank Profs. Eugene Chen (at Colorado State University) and Prof. R. Waymouth (Stanford University)[54] for valuable discussions of the similarities and differences between the problems of accounting for polymer size distribution versus PSDs.

(54) Gold, L. Statistics of Polymer Molecular Size Distribution for an Invariant Number of Propagating Chains. *J. Chem. Phys.* **1958**, *28*, 91−99.

(55) Noteworthy in the following paper are: (i) the similar approach of a disproof-based, minimalistic mechanism to start; (ii) the slow initiation, fast propagation polymerization system; (iii) the monomer addition steps in the mechanism; and (iv) the finding that such a system can lead to a relatively narrow size distribution (all features closely paralleling those in the present, nanoparticle ME-PBM study). Two major differences, however, are that (v) the underlying mechanism is fundamentally different than any in the present nanoparticle study) and (vi) a Monte Carlo, stochastic simulation had to be used due to the high polymer MWs and, hence, many monomer addition steps (versus the full ODE approach possible for our nanoparticle formation reaction and its order of magnitude fewer number of steps). Nevertheless, the following excellent work is an example that fits our definition of ME-PBM, albeit now in polymer chemistry, something that expands the scope and impact of the concept of ME-PBM. We thank Prof. Waymouth for stimulating discussion of the PBMs of polymer versus particle formation systems: Brown, H. A.; Xiong, S.; Medvedev, G. A.; Chang, Y. A.; Abu-Omar, M. M.; Caruthers, J. M.; Waymouth, R. M. Zwitterionic Ring-Opening Polymerization: Models for Kinetics of Cyclic Poly(caprolactone) Synthesis. *Macromolecules* **2014**, *47*, 2955−2963.

(56) Özkar, S.; Finke, R. G. Nanoparticle Formation Kinetics and Mechanistic Studies Important to Mechanism-Based Particle-Size Control: Evidence for Ligand-Based Slowing of the Autocatalytic Surface Growth Step Plus Postulated Mechanisms. *J. Phys. Chem. C* **2019**, *123*, 14047−14057. See also refs 1−21 therein to ligand effects in nanoparticle chemistry.

(57) Yin, C.-X.; Finke, R. G. Kinetic and Mechanistic Studies of Vanadium-Based, Extended Catalytic Lifetime Catechol Dioxygenases. *J. Am. Chem. Soc.* **2005**, *127*, 13988−13996.

DOI: 10.1021/jacs.9b06364
J. Am. Chem. Soc. 2019, 141, 15827−15839

(58) Bayram, E.; Linehan, J. C.; Fulton, J. L.; Roberts, J. A. S.; Szymczak, N. K.; Smurthwaite, T. D.; Özkar, S.; Balasubramanian, M.; Finke, R. G. Is it Homogeneous or Heterogeneous Catalysis Derived from $[RhCp^*Cl_2]_2$? *In Operando* XAFS, Kinetic, and Crucial Kinetic Poisoning Evidence for Subnanometer Rh_4 Cluster-Based Benzene Hydrogenation Catalysis. *J. Am. Chem. Soc.* **2011**, *133*, 18889−18902.
(59) Mondloch, J. E.; Wang, Q.; Frenkel, A. I.; Finke, R. G. Development Plus Kinetic and Mechanistic Studies of a Prototype Supported-Nanoparticle Heterogeneous Catalyst Formation System in Contact with Solution: Ir(1,5-COD)Cl/γ-Al_2O_3 and Its Reduction by H_2 to $Ir(0)_n/\gamma$-Al_2O_3. *J. Am. Chem. Soc.* **2010**, *132*, 9701−9714.
(60) Mondloch, J. E.; Finke, R. G. Supported-Nanoparticle Heterogeneous Catalyst Formation in Contact with Solution: Kinetics and Proposed Mechanism for the Conversion of Ir(1,5-COD)Cl/γ-Al_2O_3 to $Ir(0)_{\sim 900}/\gamma$-Al_2O_3. *J. Am. Chem. Soc.* **2011**, *133*, 7744−7756.
(61) Mondloch, J. E.; Bayram, E.; Finke, R. G. A review of the kinetics and mechanisms of formation of supported-nanoparticle heterogeneous catalysts. *J. Mol. Catal. A: Chem.* **2012**, *355*, 1−38.
(62) Morris, A. M.; Watzky, M. A.; Agar, J. N.; Finke, R. G. Fitting Neurological Protein Aggregation Kinetic Data via a 2-step, Minimal/"Ockham's Razor" Model: The Finke-Watzky Mechanism of Nucleation Followed by Autocatalytic Surface Growth. *Biochemistry* **2008**, *47*, 2413−2427.
(63) Watzky, M. A.; Morris, A. M.; Ross, E. D.; Finke, R. G. Fitting Yeast and Mammalian Prion Aggregation Kinetic Data with the Finke-Watzky Two-Step Model of Nucleation and Autocatalytic Growth. *Biochemistry* **2008**, *47*, 10790−10800.
(64) Morris, A. M.; Finke, R. G. α-Synuclein aggregation variable temperature and variable pH kinetic data: a re-analysis using the Finke-Watzky 2-step model of nucleation and autocatalytic growth. *Biophys. Chem.* **2009**, *140*, 9−15.
(65) Morris, A. M.; Watzky, M. A.; Finke, R. G. Protein aggregation kinetics, mechanism, and curve-fitting: A review of the literature. *Biochim. Biophys. Acta, Proteins Proteomics* **2009**, *1794*, 375−397.
(66) Finney, E. E.; Finke, R. G. Is There a Minimal Chemical Mechanism Underlying Classical Avrami-Erofe'ev Treatments of Phase Transformation Kinetic Data? *Chem. Mater.* **2009**, *21*, 4692−4705.
(67) Tong, F.; Hanson, M. P.; Bardeen, C. J. Analysis of reaction kinetics in the photomechanical molecular crystal 9-methylanthracene using an extended Finke-Watzky model. *Phys. Chem. Chem. Phys.* **2016**, *18*, 31936−31945.
(68) Avinash, M. B.; Sandeepa, K. V.; Govindaraju, T. Emergent Behaviors in Kinetically Controlled Dynamic Self-Assembly of Synthetic Molecular Systems. *ACS Omega* **2016**, *1*, 378−387.
(69) Oladoja, N. A. A critical review of the applicability of Avrami fractional kinetic equation in adsorption-based water treatment studies. *Desalin. Water Treat.* **2016**, *57*, 15813−15825.
(70) The above greater generality anticipated, the Achilles heel and slow step of broader applications of true ME-PBM is expected to be the discovery of the true, experimentally determined *nucleation mechanism* for a given system. Without the detailed nucleation mechanism to start the PBM out correctly, one will not have true ME-PBM nor its implied greater reliability. As noted in the main text, the otherwise powerful full ODE approach will become more and more compuationally challenging for larger and larger particle formation, especially when agglomeration is involved.
(71) Current limitations of ME-PBM and the full ODE approach that are apparent at present include the following: (i) the desire for more detailed, experimentally based mechanisms (i.e., beyond the deliberately minimum mechanisms in Scheme 3) as even better input into one's ME-PBM; (ii) the increasing computation time required for the full-ODE approach once the particles get larger and larger; and (iii) the much greater computational time required when agglomeration is part of the particle-formation process (and, hence, the difficulties to impossibility of implementing the full ODE approach where agglomeration is occurring, especially for larger final particle sizes). A full version of the present studies, aimed at assisting the reader interested in ME-PBM, is nearing completion and will be submitted for publication in due course: Handwerk, D. R.; Shipman, P. D.; Whitehead, C. B.; Özkar, S.; Finke, R. G. Particle Size Distributions via Mechanism-Enabled Population Balance Modeling, in progress.

DOI: 10.1021/jacs.9b06364
J. Am. Chem. Soc. 2019, 141, 15827−15839